Available online at www.sciencedirect.com

ScienceDirect

Procedia Engineering 199 (2017) 152–157

Procedia Engineering

www.elsevier.com/locate/procedia

X International Conference on Structural Dynamics, EURODYN 2017

Dynamic response of a damaging masonry wall

Daniela Addessi, Cristina Gatta, Fabrizio Vestroni

Department of Structural and Geotechnical Engineering, Sapienza University of Rome, Via Eudossiana 18, 00184 Rome, Italy

Abstract

A nonlocal damage-plastic model is adopted to describe the nonlinear structural response of masonry structures. The model, based on a macromechanical approach, accounts for strength and stiffness degradation with hysteretic dissipation typically characterizing the masonry response, when it is subjected to horizontal loads. The stiffness recovery due to the crack closure, under cyclic loading, is also introduced by defining two different scalar damage variables for prevailing tensile and compressive states. To explore the effect of such nonlinear phenomena on the masonry structural response, the behavior of an unreinforced slender wall is investigated in the dynamic field. Special attention is devoted to the analysis of the wall frequency response curves (FRCs), obtained by imposing base harmonic accelerations with slowly time-variable frequency. These curves highlight the complexity of the dynamic phenomenon: due to the stiffness decay exhibited by the wall, a continuous variation of its natural frequencies occurs, which in turn modifies the resonance conditions. Finally, the wall response results strongly path-dependent and the characteristics of the wall restoring force lead to multi-valued FRCs.

Peer-review under responsibility of the organizing committee of EURODYN 2017.

Keywords: Masonry; damage; plasticity; unilateral effect; cyclic response; frequency response curves.

1. Introduction

Masonry buildings represent a significant part of the historical and architectural heritage in many countries. The development of efficient numerical procedures to study their structural response especially under seismic loading conditions is a challenging and significant task for researchers and practitioners. Masonry material shows a very complex behavior due to the heterogeneous and composite nature of the medium and to the strongly nonlinear behavior of the constituents. The overall response is influenced by shape, sizes and arrangement of blocks and mortar, by the cohesion and friction between them, and by their mechanical properties. During the loading process, onset, growth and coalescence of microcracks occur and plastic irreversible strains are accumulated. Different modeling approaches, based on different scales of the analysis [1–6], have been proposed, that is micromechanical, macromechanical and multi-scale. All contain damage and plasticity constitutive laws to describe the mechanical response of each

* Corresponding author.
E-mail address: cristina.gatta@uniroma1.it

1877-7058
Peer-review under responsibility of the organizing committee of EURODYN 2017.
10.1016/j.proeng.2017.09.198

constituents or the overall response of the masonry modeled as an equivalent homogenized medium. Macromechanical approaches represent a fair compromise between accuracy of results and computational burden and are able to take into account the main mechanisms characterizing masonry response under cyclic loads: strength and stiffness degradation, unilateral effect and hysteretic dissipation. All these nonlinear mechanisms significantly affect both the static and dynamic masonry structural response, as shown both by experimental evidences and by the observation of the masonry real response under seismic events.

A number of studies have been dedicated to investigate the effects of the degrading and plasticity phenomena on the nonlinear cyclic static response of masonry walls. But the presence of damage and irreversible strains substantially modifies the dynamic structural response too, under seismic actions [4,6] and harmonic excitations [4,7]. In particular, the frequency response curves (FRCs) are relevant for the structural dynamic characterization and permit to highlight and distinguish the effects of the different nonlinear mechanisms. Several studies on nonlinear oscillators, characterized by geometrical and/or material nonlinearities, have clarified that the FRCs features are referable to the restoring force shape: hardening or softening behavior, multi-valued curves with jump phenomenon or single-valued curves can be occured [8–10].

This study adopts the damage-plastic model and the finite element formulation presented in [5] to numerically investigate the nonlinear response of an unreinforced masonry wall. The masonry constitutive model introduces two different scalar damage variables, governing the degrading processes for prevailing tensile and compressive states, to account for the unilateral effect. Moreover, a classical $J2$ formulation governs the flow of the irreversible plastic strains. First, the nonlinear static response of the wall is investigated under horizontal loads. Then, the wall dynamic response is explored by deriving the frequency response curves of the structure, exhibiting degrading and plastic mechanisms and framing the influence of the peculiar masonry constitutive relationship within the large amount of the available data devoted to systems characterized by invariant restoring forces.

2. Model and equilibrium equations

A 2D plane stress formulation under the hypothesis of small displacements and strains is adopted. The stress-strain constitutive relationship, based on the damage-plastic model presented in [5], is expressed as:

$$\boldsymbol{\sigma} = \left[(1 - D_t)\,\alpha_t + (1 - D_c)\,\alpha_c\right]^2 \mathbf{C}\,(\boldsymbol{\varepsilon} - \boldsymbol{\varepsilon}^p) \tag{1}$$

where $\boldsymbol{\sigma}$, $\boldsymbol{\varepsilon}$ and $\boldsymbol{\varepsilon}^p$ are the stress, total strain and plastic strain vectors, respectively, while $\mathbf{C}$ is the elastic constitutive matrix of the undamaged material under plane stress conditions. D_t and D_c are two distinct damage variables, measuring the material degradation for prevailing tensile and compressive states, respectively, while $\alpha_{t/c}$ are weighting coefficients defined below. The definition of two distinct damage variables in tension and compression permits to account for the unilateral effect, related to the closure in compression of the tensile cracks. According to their definition [11], D_t and D_c range in $[0, 1]$, the lower bound corresponding to the initial undamaged material state, the upper one attained when the material is completely damaged. The thermodynamic irreversible constraint is imposed, such that $\dot{D}_{t/c} \geq 0$, together with the condition $D_t \geq D_c$.

The evolution processes of the two damage variables are driven by two equivalent strain measures, Y_t and Y_c, defined as:

$$Y_t = \sqrt{\sum_{i=1}^{3} \langle e_i \rangle_+^2} \qquad Y_c = \sqrt{\sum_{i=1}^{3} \langle e_i \rangle_-^2 + \kappa \sum_{i=1}^{3} \sum_{j \neq i} \langle e_i \rangle_- \left\langle e_j \right\rangle_-} \tag{2}$$

where the Mac'Auley brackets $\langle \bullet \rangle_{+/-}$ compute the positive/negative part of a quantity, κ is a material parameter influencing the shape of the damage limit function in compression and e_i results as:

$$e_i = (1 - 2\nu)\,\hat{\varepsilon}_i + \nu \textstyle\sum_{j=1}^{3} \hat{\varepsilon}_j \tag{3}$$

$\hat{\varepsilon}_i$ denoting the principal total strains and ν the Poisson ratio. Furthermore, two damage limit functions, F_t and F_c, are defined to completely describe the damage evolution processes by means of the classical Kuhn-Tucker conditions, expressed as:

$$\begin{aligned} F_t &= (Y_t - Y_{t0}) - D_t\,(a_t Y_t + b_t) \\ F_c &= (Y_c - Y_{c0}) - D_c\,(a_c Y_c + b_c) \end{aligned} \tag{4}$$

Here, the material parameters Y_{t0} and Y_{c0} set the damage initial thresholds in tension and compression, while $b_{t/c}$ and $a_{t/c}$ influence the uni-axial tension and compression peak strengths and the softening branches slope, respectively. Finally, the weighting coefficients combining the two damage variables in Eq. (1) are defined as:

$$\alpha_t = \frac{Y_t^e / Y_{t0}}{Y_t^e / Y_{t0} + Y_c^e / Y_{c0}} \qquad \alpha_c = 1 - \alpha_t \tag{5}$$

where the principal elastic strains $\hat{\varepsilon}_i^e$ are used to evaluate $Y_{t/c}^e$, according to formulas (2) and (3).

Concerning the adopted plasticity model, a classical $J2$ model with hardening is considered, denoting with σ_y and H_k the yield stress and the kinematic hardening coefficient, respectively.

The presented model and the developed solution algorithm for the evolution problems of damage and plastic variables have been implemented in a finite element procedure (FEAP code [12]), where the mesh-dependence problem, related to strain-softening behavior, has been overcome by adopting the nonlocal regolarization technique [13]. Thus, the integral definition $\tilde{Y}_{t/c}$ and $\tilde{Y}_{t/c}^e$ of the damage associated variables is introduced in Eqs. (2,4,5).
The FE discretized equations, governing the dynamic nonlinear structural problem, are written as:

$$\mathbf{M}\ddot{\mathbf{u}} + \mathbf{D}\dot{\mathbf{u}} + \mathbf{P}^{int}(\mathbf{u}) = \mathbf{P}^{ext} \tag{6}$$

where $\mathbf{u}$, $\dot{\mathbf{u}}$ and $\ddot{\mathbf{u}}$ are the global nodal displacement, velocity and acceleration vectors, respectively, in which dots denote the derivative with respect to time. The global mass matrix $\mathbf{M}$ is assembled by following a lumped approach, while the Rayleigh damping matrix $\mathbf{D}$ is evaluated as a linear combination of the mass and initial elastic stiffness matrix. Finally, $\mathbf{P}^{ext}$ is the external force vector and $\mathbf{P}^{int}(\mathbf{u})$ is the internal force vector, accounting for the nonlinear structural response. The implicit Newmark-β algorithm is used for the integration in time of Eqs. (6) and the Newton-Raphson procedure to evaluate the solution within each time step Δt.

3. Monotonic and cyclic restoring force

The model presented in Section 2 is used to study the structural response of an unreinforced masonry wall. The geometrical parameters of the wall, schematically shown in Fig. 1(a), are height $H = 6\,\mathrm{m}$ and thickness $s = 1\,\mathrm{m}$. These have been selected to reproduce typical geometries of walls of historical buildings and churches, as for example the external walls of the Basilica S. Maria di Collemaggio [14], aiming at studying the nonlinear static and dynamic response of these slender walls taking into account damage and plasticity nonlinear phenomena. In fact, a unity wall width is set to analyze the out-of-plane response of a strip composing the external wall. Concerning the material properties, that is Young's modulus E, compression strength and volume density ρ, reference is made to experimental tests on masonry walls performed at the Joint Research Centre of Ispra [15]. Table 1 contains the adopted material parameters, corresponding to tensile and compressive uni-axial strengths equal to 0.3E+6 N/m^2 and 5E+6 N/m^2, respectively.

Table 1. Masonry material parameters.

E [N/m^2]	ν	ρ [kg/m^3]	Y_{t0}	Y_{c0}	a_t	a_c	b_t	b_c	σ_y [N/m^2]	H_k [N/m^2]
1.7E+9	0.15	1750	7E-5	9E-4	9.7E-1	9.9E-1	4.5E-4	1.6E-2	1.3E+6	$0.95E$

Considering simplified boundary conditions, where the wall is completely restrained at the base and free at the top, monotonic and cyclic loadings are applied. Fig. 1(b) shows the load-displacement global curve obtained by applying

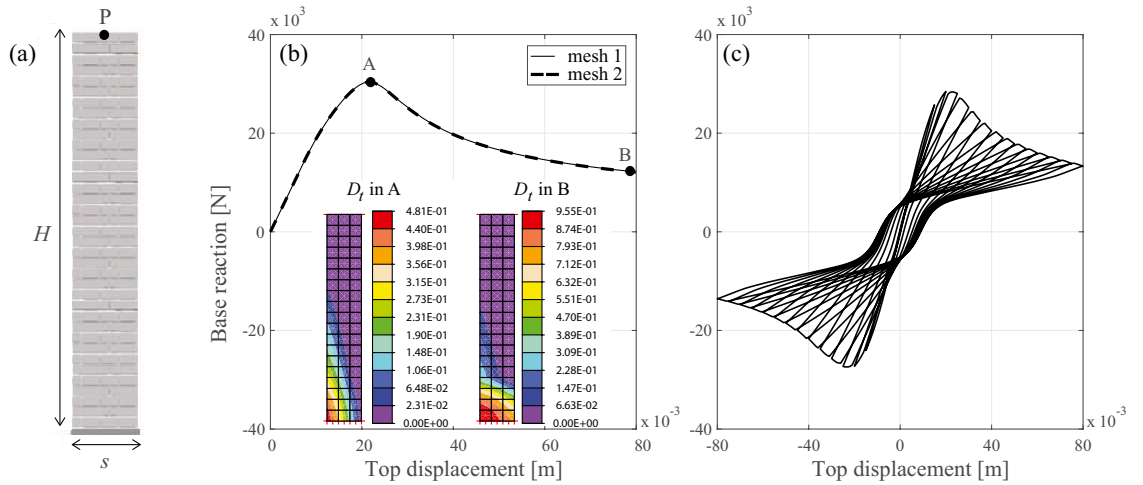

Fig. 1. (a) Schematic of the wall; (b) monotonic and (c) cyclic load-displacement global curves.

a monotonic horizontal displacement at the top side nodes. A nonlocal radius $l_c = 0.5$ m is used and two different meshes made of 19×3 (mesh 1 solid line) and 38×6 (mesh 2 dashed line) FEs are compared. The perfect agreement of the two curves confirms the effectiveness of the adopted regularization technique and, then, the coarser mesh is adopted in the following. However, the pushover response curve highlights that the structural response is strongly affected by the degrading phenomena, showing significant decay of strength and stiffness. Pushing the structure towards right, after the initial elastic branch, damage arises in the bottom left corner, where the tensile strains are concentrated and then spreads around this region. Fig. 1(b) also contains the tensile damage maps corresponding to the peak load (point A) and at the end of the analysis (point B), showing that the steep softening branch is due to the spread of damage along the entire base section. Finally, the wall response is investigated by imposing a cyclic horizontal displacement history at the top. The obtained curve, contained in Fig. 1(c), shows the onset of plastic strains as well as the stiffness recovery, under load reversal, essentially due to the opening and subsequent closing of the tensile cracks, when the material undergoes compression strain states.

4. Dynamic response

To point out the main features of the wall dynamic response, when this exhibits significant degrading and hysteresis mechanisms, the FRCs of the wall are derived by applying sinusoidal horizontal acceleration histories $\ddot{u}_g = U \sin[(\Omega(t)t]$ at the base. These are characterized by a fixed amplitude U and by an excitation frequency $\Omega(t)$ smoothly varying with linearly increasing and decreasing laws, called sweep 1 and 2, respectively. The ratio between $\Omega(t)$ and the first elastic circular frequency of wall ω_1 varies in the range $[0.2 \div 1.5]$ for sweep 1, conversely for sweep 2, as shown in Figs. 2(c) and (d) with black lines. Assuming a Rayleigh damping factor equal to 3%, the FRCs are evaluated in terms of top displacement of the point P in Fig. 1(a), by applying the two sweep loading histories.

Moreover, a suitable and summary measure of the overall tensile damage evolving in the wall is defined as follows:

$$D_t^g = \frac{\sqrt{\int_A (D_t)^2 \, dA}}{\sqrt{\int_A dA}} \tag{7}$$

where $A = H \times s$ denotes the wall area. Although this index does not provide information about the spatial distribution of the damage, it gives a good measure of the progression of the degrading process in the wall.

Figs. 2(a) and (b) show the top displacements (blue lines) exhibited by the wall under sweep 1 and 2 excitations, respectively, with reference to an imposed acceleration amplitude ratio $U/g = 0.06$ (where g denotes the gravity acceleration). The black lines refer to the elastic response of the wall depicted for comparison. It emerges that the wall structural response is strongly affected by the nonlinear phenomena. In fact, when the damage starts to evolve

in the structure, decay of the structural stiffness occurs causing in turn a decreasing of the natural frequencies. Thus, during sweep 1 excitation, as the wall frequency decreases, the forcing frequency increases and, then, the structure sharply comes out from the resonance condition and does not exhibit any further degrading process (see the D_t^g evolution in Fig. 2(c)). Conversely, in the case of sweep 2, when the driven frequency is approaching the natural wall frequency, the damage slowly increases, as a conseguence, a frequency reduction occurs, but now the variation of the wall frequency follows the same trend of $\Omega(t)$. Hence, the structure follows the resonance conditions and a longer and more severe damage progression occurs (see Fig. 2(d)). Basing on these step-by-step response curves, the FRCs are derived, by associating the displacement amplitude of each response cycle to the corresponding frequency excitation. Figs. 3(a) and (b) contain the obtained curves corresponding to the three different ratio $U/g = 0.04, 0.05, 0.06$, depicted in green, red and blue lines, respectively. The elastic FRCs (black lines) are also shown for comparison.

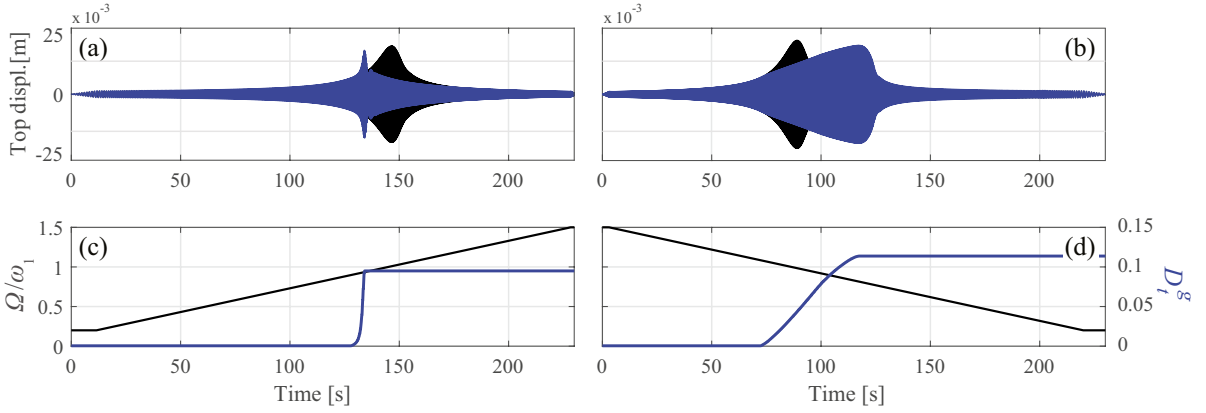

Fig. 2. Elastic (black lines) and nonlinear (blue lines) top displacement responses under (a) sweep 1 and (b) sweep 2, respectively, for $U/g = 0.06$; time histories of the global damage index (blue lines) and excitation frequency for (c) sweep 1 and (d) sweep 2.

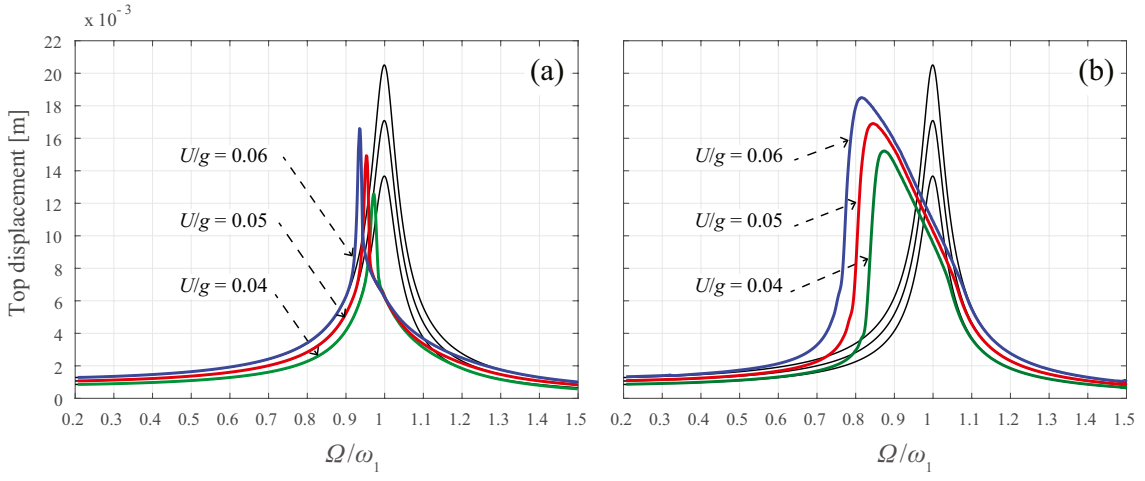

Fig. 3. FRCs for (a) sweep 1 and (b) sweep 2: elastic curves (black lines), damage-plastic curves (colored lines) for three values of U/g.

For the lower excitation amplitude, the nonlinear peak is greater than the elastic, due to damage and stiffness reduction, while by increasing the amplitude ratio U/g the peak response becomes lower than that of the corresponding elastic curves. This is due to the onset of hysteresis mechanisms. Indeed, the cyclic load-displacement curve in Fig. 1(c) shows that larger hysteresis loops are associated to larger attained displacement and, then, greater energy dissipation occurs for greater input amplitudes. As expected, the overall behavior exhibits a softening trend, as the backbone curve bents to the left with respect to the corresponding elastic one. This phenomenon can be better appreciated by Fig. 3(b) where the decreasing sweep allows for explore the points of the peak response by obtaining

the frequency-amplitude curve (backbone). Furthermore, the curves obtained under sweep 1 and 2 do not overlap, due to the strong dependence of the structural response on its stiffness decay, being path-dependent and resulting in multi-valued FRCs. In other words, the irreversible degradation of the wall mechanical properties of the wall definitely influences the dynamic amplification of the response. It is worth noting that, neglecting the damage effects and considering only an elastic-plastic constitutive response, according to the adopted $J2$ model, the same curve is obtained by applying sweep 1 and 2. This is typical of hysteretic responses not undergoeing unstable periodic solutions [8].

5. Conclusions

An isotropic nonlocal damage-plastic model has been adopted to describe the main features of the highly nonlinear mechanical response of masonry structures, under static and dynamic loading conditions. In particular, a slender masonry wall has been studied with the aim of characterizing the effects of degrading and hysteretic mechanisms on masonry structural elements typical of historical buildings. The numerical simulations have highlighted the following main features: the global cyclic load-displacement response curve of the wall shows strength and stiffness degradation, hysteretic dissipation and recovery of stiffness due to the closing in compression of the tensile cracks. Such nonlinear phenomena definitely affect the wall dynamic response. In fact, the resonance condition continuously changes in relation with the decay of the structural stiffness, causing a variation of the natural frequencies. The FRCs, evaluated by imposing base harmonic accelerations with slowly increasing and decreasing frequency, highligthed a strong differences of the structural behavior with respect to the steady-state response of nonlinear invariant systems. The curves show a softening trend and a peculiar multi-valued aspect, typical of the systems with restoring force characterized by not fully hysteresis. Besides, the equilibrium points of the FRCs are strongly dependent on the history due to the irreversible effect of the damage, preventing to retrace the same curve.

Acknowledgements

This work has been partially supported by the Project 2015TTJN95 'Identification and Monitoring of Complex Structural Systems'.

References

[1] D. Addessi, S. Marfia, E. Sacco, J. Toti, Modeling Approaches for Masonry Structures, The Open Civ. Eng. J. 8 (2014) 288–300.
[2] D.V. Oliveira, P.B. Lourenço, Implementation and validation of a constitutive model for the cyclic behaviour of interface elements, Comput. Struct. 82 (2004) 1451-1461.
[3] L. Karapitta, H. Mouzakis, P. Carydis, Explicit finite-element analysis for the in-plane cyclic behavior of unreinforced masonry structures, Earthquake Engng Struct. Dyn. 40 (2011) 175–193.
[4] J. Toti, V. Gattulli, E. Sacco, Nonlocal damage propagation in the dynamics of masonry elements, Comput. Struct. 152 (2015) 215–227.
[5] D. Addessi, G. Gatta, F. Vestroni, Static and dynamic nonlinear response of masonry walls. Submitted
[6] L. Gambarotta, S. Lagomarsino, Damage models for the seismic response of brick masonry shear walls. Part II: the continuum model and its applications, Earthquake Engng Struct. Dyn. 26 (1997) 441–462.
[7] D. Addessi, E. Cappelli, C. Gatta, F. Vestroni, Out-of-plane dynamic response of a tuff masonry wall: shaking table testing and numerical simulation, in: M. Papadrakakis, M. Fragiadakis (Eds.), 6^{th} ECCOMAS Thematic Conference on Computational Methods in Structural Dynamics and Earthquake Engineering, Rhodes Island, 2017.
[8] D. Capecchi, F. Vestroni, Periodic response of a class of hysteretic oscillators, Int. J. Nonlinear Mech. 25 (1990) 309–317.
[9] C.W. Wong, Y.Q. Ni, J.M. Ko, Steady-State Oscillation of Hysteretic Differential Model. II: Performance Analysis, J. Eng. Mech. 120 (1994) 2299–2325.
[10] W. Lacarbonara, F. Vestroni, Nonclassical Responses of Oscillators with Hysteresis, Nonlinear Dyn. 32 (2003) 235–258.
[11] L.M. Kachanov, Time of rupture process under creep conditions, Izvestia Akademii Nauk, Otd Tech Nauk, 8, 26-31, 1958.
[12] R.C. Taylor, FEAP-A finite element analysis program, Version 8.3. Department of Civil and Environmental Engineering. University of California at Berkeley, 2011.
[13] P. Pijaudier-Cabot, Z.L. Bazant, Non local damage theory, J. Eng. Mech. ASCE 118 (1987) 1512–1533.
[14] V. Gattulli, E. Antonacci, F. Vestroni, Field observations and failure analysis of the Basilica S. Maria di Collemaggio after the 2009 LAquila earthquake, Eng. Fail. Anal. 34 (2013) 715–734.
[15] A. Anthoine, G. Magonette, G. Magenes, Shear-compression testing on analysis of brick masonry walls, in: Duma(Ed), 10th European Conference on Earthquake Engineering, 1995, vol 3, pp. 1657-1662.